Prediction of the equilibrium moisture content based on the chemical composition and crystallinity of natural fibres

Sweygers , Nick ; Depuydt, Delphine E.C. ; Eyley, Samuel ; Thielemans, Wim ; Mosleh, Yasmine; Ivens, Jan; Dewil, Raf; Appels, Lise ; Van Vuure, Aart Willem

DOI
10.1016/j.indcrop.2022.115187

Publication date
2022

Document Version
Final published version

Published in
Industrial Crops and Products

Industrial Crops & Products 186 (2022) 115187

Contents lists available at ScienceDirect

Industrial Crops & Products

journal homepage: www.elsevier.com/locate/indcrop

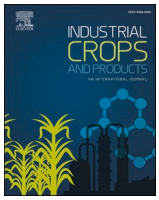

Prediction of the equilibrium moisture content based on the chemical composition and crystallinity of natural fibres

Nick Sweygers [a,*], Delphine E.C. Depuydt [b], Samuel Eyley [c], Wim Thielemans [c], Yasmine Mosleh [d], Jan Ivens [e], Raf Dewil [a], Lise Appels [a], Aart Willem Van Vuure [b]

[a] KU Leuven, Department of Chemical Engineering, Process and Environmental Technology Lab, J. De Nayerlaan 5, 2860 Sint-Katelijne-Waver, Belgium
[b] KU Leuven, Department of Materials Engineering, Composite Materials Group, Kasteelpark Arenberg 44, 3001 Leuven, Belgium
[c] KU Leuven, Department of Chemical Engineering, Renewable materials and nanotechnology research group, campus Kulak Kortrijk, Etienne Sabbelaan 53, 8500 Kortrijk, Belgium
[d] TU Delft, Department of Civil Engineering and Geosciences, Biobased Structures and Materials, Kluyverweg 1, 2629 HS Delft, Netherlands
[e] KU Leuven, Department of Materials Engineering, Composite Materials Group, J. De Nayerlaan 5, 2860 Sint-Katelijne-Waver, Belgium

ARTICLE INFO

Keywords:
Natural fibres
Equilibrium moisture content
Crystallinity
Chemical composition

ABSTRACT

Natural fibre-based materials offer various advantages compared to synthetic fibres, however their applications are limited mainly due to their hygroscopic properties, which are affected by their chemical composition, microstructure and the porosity of the plant cells of which the fibre is composed. Therefore, this work investigates the hygroscopic behavior of natural fibres to obtain a better understanding of the relation of the chemical composition of the fibres, their crystallinity, and their equilibrium moisture content. The crystallinity index was determined to include amorphous cellulose into the developed models. Nine biomass samples were selected (flax, hemp, jute, spruce, bamboo, corn stalks, palm leaves, rice husk and wheat straw) to construct models via linear regression to predict the moisture sorption behavior of natural fibres. Thorough statistical (ANOVA, RMSE) analysis showed that the developed models are relevant and descriptive. From all major plant cell wall constituents (lignin, crystalline cellulose, amorphous cellulose and hemicellulose), it is hemicellulose's hygroscopicity that is largely responsible for the moisture uptake of the fibres, with (amorphous) cellulose and lignin playing a (much) smaller role. This study has improved the understanding of the hygroscopic behavior of natural fibres, and is important for optimal application of these fibres in composite materials.

1. Introduction

Nature provides a variety of natural fibres that can be used for composite applications (Müssig, 2010; Bourmaud et al., 2018; Faruk et al., 2014; Azwa et al., 2013; Savic et al., 2020; Cheng et al., 2021; Liu and Tisserat, 2018; Liuzzi et al., 2020). Natural fibre reinforced composites can compete with synthetic glass fibre reinforced composites (J. G. and CELC, 2018; Manian et al., 2021; Shahinur et al., 2022), and show a number of benefits - low density, good specific mechanical properties, originating from renewable resources, low cost, etc. - that make them attractive to replace more traditional materials. However, there are still a few disadvantages linked to the use of natural fibres: their higher moisture absorption, associated lower durability, greater variability and limited processing temperatures. One of the challenges natural fibre reinforced composites face, is to reduce moisture-induced degradation (Azwa et al., 2013; Liu and Tisserat, 2018). Natural fibres absorb water, which results in dimensional changes of the fibres, and once embedded in a composite, this can degrade the fibre-matrix interface, resulting in a loss in composite properties. To improve the moisture resistance of natural fibres, more insight into the moisture absorption is needed (Wei et al., 2022).

One way to study the moisture sorption behaviour of natural fibres is by dynamic vapour sorption measurements (DVS), as in the work by Hill et al. (2009). where several moisture sorption curves for different natural fibers were measured. From this work it becomes clear that different fibers show different sorption behaviour with different equilibrium moisture content (EMC). The EMC is reached when the amount of water molecules arriving at the surface equals the amount of molecules leaving the surface (Time, 1998). Hill et al. (2009). studied the sorption behaviour of a range of natural fibres and concluded that the EMC

* Corresponding author.
E-mail address: nick.sweygers@kuleuven.be (N. Sweygers).

https://doi.org/10.1016/j.indcrop.2022.115187
Received 25 March 2022; Received in revised form 22 May 2022; Accepted 5 June 2022
Available online 13 June 2022

seemed to be higher for fibres with high lignin content. They hypothesized that this might be related to the ability of the lignin network to deform to accommodate water within the cell wall. Rautkari et al. (2013) studied the role of the accessibility of hydroxyl groups in controlling the moisture content in wood, based on deuterium exchange in a DVS. They found a poor relation between the EMC and the number of hydroxyl groups and concluded that there must be an additional mechanism that helps to control the EMC.

Natural fibres are built up out of three main constituents: cellulose, hemicellulose and lignin, each with their own specific function. Cellulose is a linear carbohydrate polymer consisting of many glucose units which form the framework of the plant (Douglas et al., 2013). It can be structured into crystalline microfibrils, which are located within the fibre cell wall. These microfibrils are responsible for the strength, stiffness and structural stability of the fibre (Salmén and Bergström, 2009). Cellulose has three hydroxyl groups (OH), which are possible sites for hydrogen bonds, making it highly hygroscopic. However, the sensitivity to water is severely lowered when cellulose stacks to form crystalline regions (Müssig, 2010; Douglas et al., 2013; Rowell, 2005; Salmén, 2015). In the plant, the crystalline regions are alternated with dislocated cellulose regions (Salmén and Bergström, 2009), which are obviously more moisture sensitive because of increased free volume.

Hemicellulose is a branched carbohydrate polymer, containing five and six carbon sugars (Kabir et al., 2012; T. A. and Abdul, 2013). It occurs mainly in the primary cell wall, middle lamellae and secondary layer of the plant where it is hydrogen bonded with cellulose and acts as support material for the microfibrils (Müssig, 2010; Kabir et al., 2012). Hemicelluloses have a more open structure than cellulose and are therefore more hydrophilic as well as soluble in water. They are also sensitive to thermal degradation.

Lignin is characterised by aromatic rings and has an amorphous structure. It is deposited in the remaining spaces in the cell wall and between the cells, when the cellulose and hemicelluloses have already been formed (Blackwell and Walker, 2006). In this way it gives the plant extra resistance to compressive forces. Covalent bonds between hemicellulose and lignin have been proposed to exist in wood and are referred to as the lignin-carbohydrate complexes (LCC) (Lawoko et al., 2005; Giummarella and Lawoko, 2016). Lignin, made up out of aromatic rings and aliphatic chains, is more hydrophobic than cellulose and hemicellulose and, therefore, it is believed to improve water resistance (Douglas et al., 2013). Though lignin is a complex 3D molecule, it is constructed from three simple precursors: p-coumaryl acohol (H), coniferyl alcohol (G) and sinapyl alcohol (S). S lignin contains a higher amount of methoxyl groups, limiting the crosslinking of lignin (Douglas et al., 2013). Due to this lower degree of crosslinking, effects might be expected on the glass transition temperature with changing S/G ratio; this was investigated by Horvath et al (Horvath et al., 2011)., who found that the glass transition temperature was not affected by the structure of lignin but was purely related to the absolute lignin content.

Other minor polysaccharides present in the plant are pectins and starch. Pectin is a carbohydrate akin to hemicellulose, and is an important component of the middle lamella (Bourmaud et al., 2018). Pectin is also hydrophilic and water-soluble. Starch is the reserve polysaccharide of the plant, and can be found as granules in the cavities (Rowell, 2005). Besides these components, small amounts of other organic (extractives) and inorganic (ash) components can be found in natural fibres. Other non-structural extractives can be proteins, tannins, waxes, etc (Douglas et al., 2013). In wood, the hygroscopicity is generally lower the higher the amount of extractives (Young, 1985; Vahtikari et al., 2017). Ash is the general name for the inorganic compounds, left after combustion at high temperature in the presence of oxygen. One main ash component is silica, which poses problems for cutting and machining of e.g. wood (Shmulsky and Jones, 2011). The influence of extractives and ash content is not studied in this work.

Though it is generally accepted that the chemical components present in natural fibers can be ranked according to their sensitivity to moisture uptake as follows: hemicellulose > non-crystalline cellulose > lignin > crystalline cellulose (Baillie, 2000), none of the research so far attempts to correlate this with the EMC. In this work, we investigated the influence of the main natural fibre constituents on the EMC, in order to gain deeper understanding in the relationship between the equilibrium moisture content and the chemical composition and/or crystallinity of the fibre.

As mentioned, crystalline cellulose does not absorb water, unlike non-crystalline cellulose which is the second most sensitive constituent. For this reason it is interesting to determine the fraction of non-crystalline cellulose. Different techniques and analysis methods are applicable to determine the crystallinity of lignocellulosic materials. This crystallinity equals the amount of crystalline cellulose, as cellulose is expected to be the only crystalline constituent (Thygesen et al., 2005).

Native cellulose refers to cellulose as it is found in pristine plant cell walls; it is also called Cellulose I (Douglas et al., 2013). Native cellulose consists of a blend of crystals with Iα and Iβ lattice conformation, dependent on the plant source, where Iβ is considered the form being most representative of native crystalline cellulose (Douglas et al., 2013). There are different techniques to measure the CI of cellulosic material, though XRD and solid state ^{13}C NMR are most widely used. In the work of Thygesen et al. (2005)., 4 different methods were compared to assess the crystalline contribution to a cellulose diffraction pattern. It was shown that the Segal method (based on the intensity measured at two points in the diffractogram), which is still most used because of its simplicity, overestimates crystallinity. This was also concluded by Park et al. (2010). and Ahvenainen et al. (2016). The most consistent and reliable method to determine the crystallinity of plant fibre samples was determined to be Rietveld refinement (Thygesen et al., 2005). It requires knowledge of a structural model, which was published for Cellulose Iβ by Nishiyama et al. (2003), and can be used to fit the crystalline contribution including all crystalline diffraction peaks.

Another factor that has been reported to influence the hygro-expansion of paper fibre is the microfibril angle (MFA). Each elementary fibre (single fibre cell) has its own layered structure, consisting of a primary and a secondary wall. The structure of the secondary wall can vary from fibre to fibre, as illustrated in the work of Bourmaud et al. (2018). The thickest layer of the secondary wall, S2, largely determines the mechanical properties of the fibre. Therefore, the orientations of the microfibrils in that layer are crucial. The cellulose microfibrils are arranged in a helix configuration and the angle they make with the longitudinal axis is called the MFA. This angle varies for different types of fibres and is closely linked with the function of the fibre. For fibres that need to withstand high bending forces (like flax or bamboo) the MFA is low, giving high strength and stiffness to the plant. For fibres with a more protective role, e.g. coir or cotton fibres, where the role is to protect the fruit when falling down, the MFA is high to increase impact performance (Bourmaud et al., 2018). The MFA will control the shrinkage ratios in the longitudinal and transverse directions (Lindner, 2018). However, from the literature it is not clear whether it will play a role in the absolute amount of moisture sorption of the fibre. In this research, the MFA is not studied further.

In this work, the EMC is determined of different natural fibres and correlated with the experimentally determined chemical composition and crystallinity. A model, linking the amount of amorphous cellulose, hemicellulose and lignin to the EMC is proposed. The initial hypothesis of this work is that biomass with a relatively high amount of hygroscopic components (i.e. hemicellulose and amorphous cellulose) compared to hydrophobic components (i.e. lignin and crystalline cellulose) will have different EMC mainly due to hydroxyl accessibility. Based on findings in the literature, that the number of accessible hydroxyl groups differs among cellulose, hemicellulose, and lignin, we hypothesize that biomass composition will affect the EMC (Zhou et al., 2016; Yang et al., 2018; Engelund et al., 2013).

Table 1
Literature overview of the chemical composition and crystallinity of natural fibres.

	Cellulose (%)	Hemicellulose (%)	Lignin (%)	Extractives (%)	Ash (%)	CI_{XRD} (%)	References
Flax	75.9	14.4	5.8	4.7	1.6	45.8	(Hill et al., 2009; Morin et al., 2021; Moryganov et al., 2018)
Hemp	81.5	11.0	4.4	5.0	1.5	35.7	(Hill et al., 2009; Morin et al., 2021; Stevulova et al., 2014)
Jute	61.0–65.2	14–22.2	10.8–12	0.5–1.5	0.5–2.0	58.9	(Hill et al., 2009; Biswal et al., 2019; Gupta and Srivastava, 2015; Bashar et al., 2019)
Spruce	24.7–44.8	6.0	31.5	3.7–23.4	5.5	46.0	(Hill et al., 2009; Skulcova et al., 2018; Monavari et al., 2009; Ku et al., 2007; Le Normand et al., 2014)
Bamboo	40.7–50	20–26.5	20–30	2.5–5	1.2	48.0	(Kumar, 2018; Leenakul and Tippayawong, 2010; Hamdan, 2020)
Corn	29.4–31.7	17.9	33.6	12.6–18.5	0.9–4.3	58.2	(Govil et al., 2020; Guo et al., 2018; Liu et al., 2019)
Palm leaves	24.6–44.5	18.8–36.6	14.6–27.4	20.1 – 32.9	5.4–6.0	38.0	(Ahmad et al., 2011; Nasser et al., 2016; Arnata et al., 2019; Adam et al., 2018; Owolabi et al., 2016; Khattab and El, 2018)
Rice husk	22.7–40.2	10.9–19.7	14.4–33.9	3.2–10.2	15.3 – 16.8	62.3	(Chen et al., 2014; Effendi et al., 2019; João et al., 2020; Gullón et al., 2011)
Wheat straw	35.9–40.5	17.2	18.9–23.3	7.62–15.9	5.8–7.6	50.0	(Yelle et al., 2013; Tozluoğlu et al., 2015; Özyürek and van Heiningen, 2018; Lu et al., 2018)

2. Materials and methods

2.1. Sorption behaviour

Moisture sorption curves of all evaluated natural fibres - bamboo (Belgium), flax (Belgium), hemp (France), jute (India), spruce (Belgium), corn (Belgium), palm leaves (Tunisia), rice husk (Italy) and wheat straw (Belgium) - were measured via an automated gravimetric Dynamic Vapour Sorption (DVS) analyser from Surface Measurement Systems at isothermal temperature of 21 °C. The uptake of the water vapour was determined gravimetrically using a high precision balance with a mass resolution of ± 0.1 μg. The relative humidity around the sample was controlled by mixing saturated and dry gas streams using mass flow controllers.

The benefit of this technique is the control over both the relative humidity (RH) and the temperature (i.e. 21 °C). The fibres were milled prior to measurement, to a powder with a size < 250 μm. Approximately 5–10 mg of the natural fibre dust was used. The sample was first dried to a relative humidity of 0%; subsequently, the humidity was changed in steps of 5% RH, (0, 5, 10, 15 … 85, 90, 95%). Every subsequent step was initiated when the change of the sample mass versus time was less than 0.02%/min. A desorption curve with equal levels of RH was realised up to full desorption. The moisture content was calculated according to Eq. (2):

$$MC \quad \% = \quad \frac{m_{eq} - m_d}{m_d} * 100 \tag{1}$$

where m_{eq} is the mass of the sample at equilibrium and m_d the mass of the dry sample reached after the first drying stage. From the sorption curves the datapoints in the desorption and absorption cycle at a RH of 50% are used for the analysis and comparison of the different fibres.

2.2. Biomass composition

To determine the biomass composition, i.e. the lignin, cellulose and hemicellulose content, an adapted Van Soest method in-house developed by Sweygers et al (Sweygers et al.,). was used. Fibres were milled to powder in the same way as described for the DVS measurements, the measurements were performed in triplicate. In short, a first fraction, the so-called “soluble” fraction or extractives, is determined by an extraction step with a neutral detergent at 100 °C using microwave irradiation. The residual particulate matter is subsequently treated with sodium chlorite and acetic acid at 75 °C. The loss in particulate matter is attributed to the lignin fraction. The remaining solid matter is holocellulose (hemicellulose + cellulose). In a final extraction step with a mildly acidified detergent at 100 °C using microwave irradiation, hemicellulose is extracted, hence only leaving cellulose as the sole particulate matter. The ash content is determined by heating the bamboo particles for 2 h at 550 °C in a muffle furnace. The residual inorganic matter is the ash content. As a benchmark the chemical composition of 3 cellulose materials was determined via the same method. Whatman paper Grade 1, cellulose powder for column chromatography (SA – 22183, Sigma Aldrich) and medium cellulose fibres (SA – C6288, Sigma Aldrich) were selected for this.

2.3. Crystallinity

X-ray scattering data was collected on a Xenocs Xeuss 2.0 compact laboratory beamline equipped with a monochromated, point-collimated copper Kα (λ = 0.154189 nm) X-ray source operating at 0.6 mA emission current. The fibre ‘powder’ was compressed into a pellet using a hydraulic press prior to measurements. The beam path and sample chamber were under vacuum (0.4 mbar) during data collection. Diffraction patterns were collected over an angular range of 2 – 56° 2θ using a Dectris EIGER 1 M 2D detector, with a collection time of 30 min.

Table 2
Experimental data on chemical composition, crystallinity, EMC desorption and absorption, for selected natural materials.

	Cellulose (%)	Hemicellulose (%)	Lignin (%)	Extractives (%)	Ash (%)	Crystallinity (%)	EMC desorption (%)	EMC absorption (%)
Flax (Fibre)	77.1 ± 0.5	12.7 ± 0.6	2.1 ± 0.7	6.9 ± 0.1	1.2 ± 0.1	57	9.0	7.2
Hemp (Fibre)	82.1 ± 1.1	6.8 ± 0.5	2.7 ± 0.4	8.1 ± 0.2	0.2 ± 0.1	34	10.0	7.4
Jute (Fibre)	65.5 ± 0.5	15.6 ± 0.4	13.6 ± 0.3	4.9 ± 0.3	0.4 ± 0.1	44	11.0	8.4
Spruce (Fibre)	51.1 ± 0.1	15.6 ± 0.3	25.5 ± 0.4	7.4 ± 0.1	0.4 ± 0.1	31	11.5	7.0
Bamboo (Fibre)	54.9 ± 1.2	8.2 ± 0.6	19.7 ± 0.9	11.6 ± 1.2	5.5 ± 0.1	44	8.8	6.1
Corn	28.9 ± 1.3	17.9 ± 0.1	28.2 ± 1.5	19.1 ± 1.9	5.9 ± 0.5	35	9.7	7.8
Palm leaves	34.4 ± 0.7	35.8 ± 0.3	19.2 ± 1.2	5.5 ± 0.5	5.1 ± 0.2	31	16.8	13.1
Rice husk	39.4 ± 1.0	8.5 ± 1.1	30.4 ± 1.3	6.4 ± 0.3	15.2 ± 0.1	29	9.7	6.9
Wheat straw	37.3 ± 1.0	14.5 ± 1.0	29.1 ± 0.9	12.8 ± 1.3	6.3 ± 0.5	39	11.2	7.5

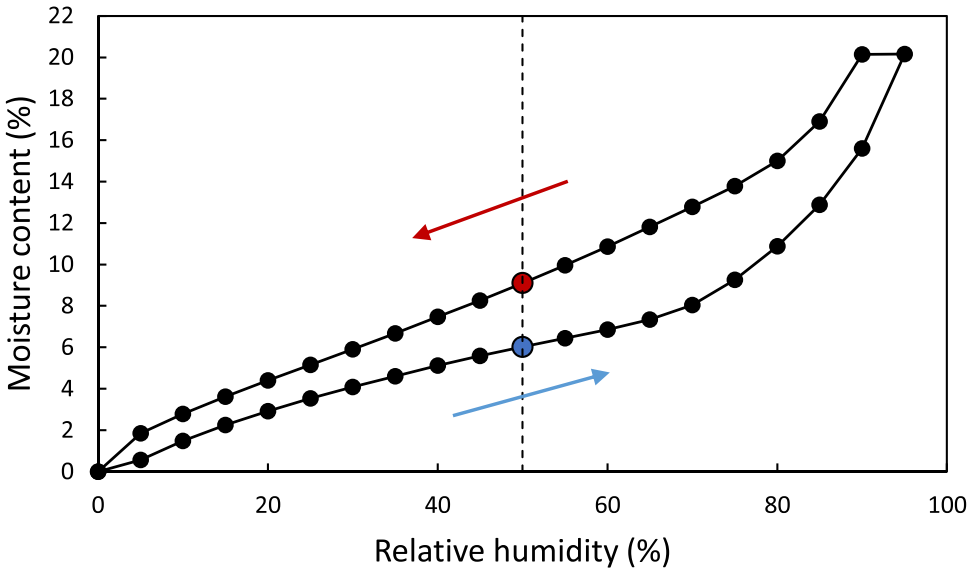

Fig. 1. Results of the DVS experiment for the bamboo fibre sample, showing the absorption (blue arrow) and desorption (red arrow) curve, measured for different RH. The points used for the calculation (RH 50%) in the desorption and absorption cycles are highlighted in red and blue respectively.

The scattering angle was calibrated by the measurement of LaB_6 under identical conditions. Data reduction was performed with Foxtrot (Xenocs/Synchrotron de Soleil).

Rietveld refinement was carried out on the cellulose Iβ structure published by Nishiyama et al. (2003). using Topas Academic v6 software with subtraction of instrumental background (collected using an empty sample holder). First refinement of a, b, γ, a scale factor, a March-Dollase preferred orientation parameter ((**0 0 4**) direction), a two-parameter background and a Lorentzian size broadening (limited to min. of 2 nm) parameter was performed on the cellulose Iβ crystal structure.

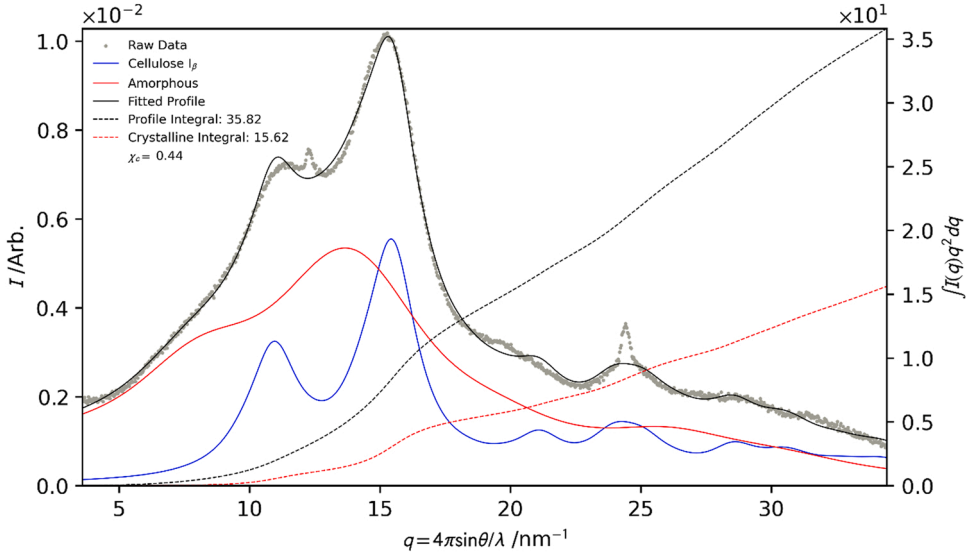

Fig. 2. Results of the raw and processed XRD data for the bamboo fibre sample, showing the crystalline cellulose Iβ and the amorphous content. Xc was calculated according to Eq. (3).

Then, an amorphous phase was added, consisting of hkls generated from a tetragonal structure (space group P4, a = 1.5 nm, c = 70 nm) to give equally spaced peaks. The peak width of the amorphous phase was limited to represent a maximum crystallite size of 1.5 nm, resulting in a broad profile similar to the expected amorphous material.

The crystallinity index was then determined using the method described by Thygesen et al. (2005). whereby the crystalline and amorphous contributions to the diffraction pattern are determined by integration of the fitted profile. The Crystallinity Index is then calculated according to Eq. (3) where I_C is the crystalline intensity, q is the scattering vector, and q0 and q1 represent the scattering vector at the respective start and end 2θ of the analysis.

$$CI = \quad X_c = \quad \frac{\int_{q0}^{q1} I_c(q)q^2dq}{\int_{q0}^{q1} I(q)q^2dq} \tag{2}$$

Supplemented with data from literature a data set was created as shown in Table 4.2.1. The equilibrium moisture content was determined from the moisture desorption and absorption curve at a relative humidity (RH) of 50% according to the work of Hill et al. (2009). Values for the chemical composition of the fibres and the crystallinity were compared with the literature (Müssig, 2010; Chand and Fahim, 2008; Mwaikambo and Ansell, 2002; John and Sabu, 2012). Crystallinity being determined as the amount of crystalline cellulose in 100 g dry material. A linear law is fitted through the data, either with one or multiple factors.

3. Results and discussion

3.1. Datasets the chemical composition and crystallinity of natural fibres

Table 1 gives an overview of the data available in literature on the chemical composition, crystallinity and moisture sorption of natural fibres. The chemical components present in natural fibres are moisture sensitive, ranked from the highest contributor to the lowest one: hemicellulose, non-crystalline cellulose, lignin and crystalline cellulose (Baillie, 2000). The amount of non-crystalline cellulose can be calculated by subtracting the crystallinity amount from the cellulose content. However, this value is not found in literature. When considering the data from literature it can be seen that all of the studies dealing with the crystallinity of these fibers exclude the determination of the chemical fiber composition. Comparison across the different studies (on crystallinity and on chemical composition) shows that for a few cases the crystallinity exceeds the total amount of cellulose. This is not possible, and the strange result can be attributed to the fact that the chemical composition and crystallinity were not determined in the same work, using different fibres, as well as the different techniques used to determine both and the errors linked to these techniques. Therefore the authors decided to redo the measurements on 9 selected natural fibres. An adapted Van Soest method was used to determine the chemical composition of the fibres and X-ray scattering with Rietveld refinement was selected as the most appropriate method to fit the crystal structure, as mentioned in the work of Thygesen et al. (2005). DVS experiments were performed to determine the EMC of each fibre. The results from the measurements are listed in Table 2. Figs. 1 and 2 show the results for the sorption experiment and the crystallinity determination for the bamboo fibre sample.

The percentage of cellulose found for the benchmark samples, ranged between 97.4% and 98.0%. Therefore the error on the chemical characterisation is supposed to be smaller than 2.5%. Sweygers et al. (2018). investigated the classical Van Soest method to analyse agricultural residues and based on the results proposed an adapted method. This new method was proven to show higher accuracy by incorporating continuous stirring into the analysis.

Comparing the measured crystallinity with the cellulose content of the samples, it is possible that a method based on the reflection measurement overestimates the crystallinity whereas the transmission method gives realistic values, since the crystallinity is for all fibres smaller than the cellulose content. In this research transmission measurements have been applied. Differences between the reflection and transmission measurement can be due to various factors (Terinte et al., 2017): 1) the effective absorption factors differ between the two geometries, 2) differences in preferred orientation between both geometries, 3) the sample height displacement error was neglected in the reflection geometry, and 4) broad peaks in the lignocellulosic samples make it hard to distinguish between small crystallites and non-crystalline material. How each of these factors influence the results measured by either reflection or transmission is still subject of research.

Another analysis technique which is emerging is the use of an internal standard (Zevin and Kimmel, 1995). In this case, a standard material with known crystallinity is mixed in known quantity with the powder of interest. In this way the accuracy of the quantisation of the crystallinity can be increased. The standard material needs to fulfil a few criteria in order to avoid bias in the measurements. It needs to be inert under X-ray radiation, have similar absorption characteristics as the material of interest and possess sharp crystalline peaks that do not overlap with the peaks of the material analyzed. For lignocellulosic

Table 3
ANOVA of the proposed models for EMC desorption and absorption (RH50).

EMC DESORPTION					
Source	DF	Sum of Squares	Mean Square	F-value	p-value
Regression	3	1100.88	366.961	330.28	0.000
Lignin	1	35.84	35.841	32.26	0.001
Hemicellulose	1	110.24	110.237	99.22	0.000
Amorphous cellulose	1	66.53	66.526	59.88	0.000
Error	6	6.67	1.111		
Total	9	1107.55			
Regression	3	1101.51	367.169	364.57	0.000
Lignin	1	16.75	16.747	16.63	0.007
Hemicellulose	1	71.7	71.7	71.19	0.000
Cellulose	1	67.15	67.15	66.67	0.000
Error	6	6.04	1.007		
Total	9	1107.55			
EMC ABSORPTION					
Source	DF	Sum of Squares	Mean Square	F-value	p-value
Regression	3	593.418	197.806	189.53	0.000
Lignin	1	9.963	9.963	9.55	0.021
Hemicellulose	1	79.678	79.678	76.34	0.000
Amorphous cellulose	1	31.909	31.909	30.57	0.001
Error	6	6.262	1.044		
Total	9	599.68			
Regression	3	595.648	198.549	295.45	0.000
Lignin	1	3.354	3.354	4.99	**0.067**
Hemicellulose	1	53.842	53.842	80.12	0.000
Cellulose	1	34.139	34.139	50.8	0.001
Error	6	4.032	0.672		
Total	9	599.68			
Regression	2	592.294	296.147	280.67	0.000
Hemicellulose	1	113.218	113.218	107.3	0.000
Cellulose	1	40.7	40.7	38.57	0.000
Error	7	7.386	1.055		
Total	9	599.68			

Table 4
Statistical analysis of the fit.

	S	R-square	R-square adjusted
Eq. 3	1.05407	99.40	99.10
Eq. 4	1.00356	99.45	99.18
Eq. 5	1.02161	98.96	98.43
Eq. 6	1.02720	98.77	98.42

materials, it is not easy to find such a standard since the mass attenuation coefficient (μ *) is very low (~0.2 cm^2/g for cellulose). De Figueiredo and Ferreira (2014). measured the amorphous amount of microcrystalline cellulose using corundum (Al_2O_3) as an internal standard, μ * = 32 cm^2/g. This is an approach that is highly interesting, and could be considered for this work as well, to verify the absolute content of amorphous material. For now, the analyses will be based on the results obtained via transmission.

3.2. Multifactor fit

The linear correlation of the three independent variables (amorphous) cellulose, hemicellulose and lignin were estimated via an analysis of variance (ANOVA) and proved to be significant (as illustrated by the p-values in Table 3, which are all lower than 0.05). This resulted in the relationships expressed by Eqs. (5) and (7). However, it should be pointed out that this fit will be skewed because of the incorporation of the crystalline cellulose in the cellulose content. This can be fixed by including non-crystalline cellulose content in the model instead of total cellulose content (via crystallinity measurements) leading to to Eqs. (4) and (6). The coefficients give a weight to the contribution of each constituent. It is known that some chemical constituents of the fibres are more prone to moisture sorption than others. This seems to be reflected in the coefficients found in this research, where hemicellulose has the highest contribution for the experimental data fit, as would be expected from literature (Baillie, 2000; Yang et al., 2018; Cermák et al., 2022; Wang et al., 2020; Yao et al., 2019).

The ANOVA analysis with the yield of EMC desorption and absorption as response is shown in Table 3. The obtained models are:

$$EMC\ \ desorption = 0.1492\ \ \boldsymbol{amorphous}\ \ \boldsymbol{cellulose}\ \ content + 0.3659\ \ hemicellulose\ \ content + 0.1581\ \ lignin\ \ content \quad (3)$$

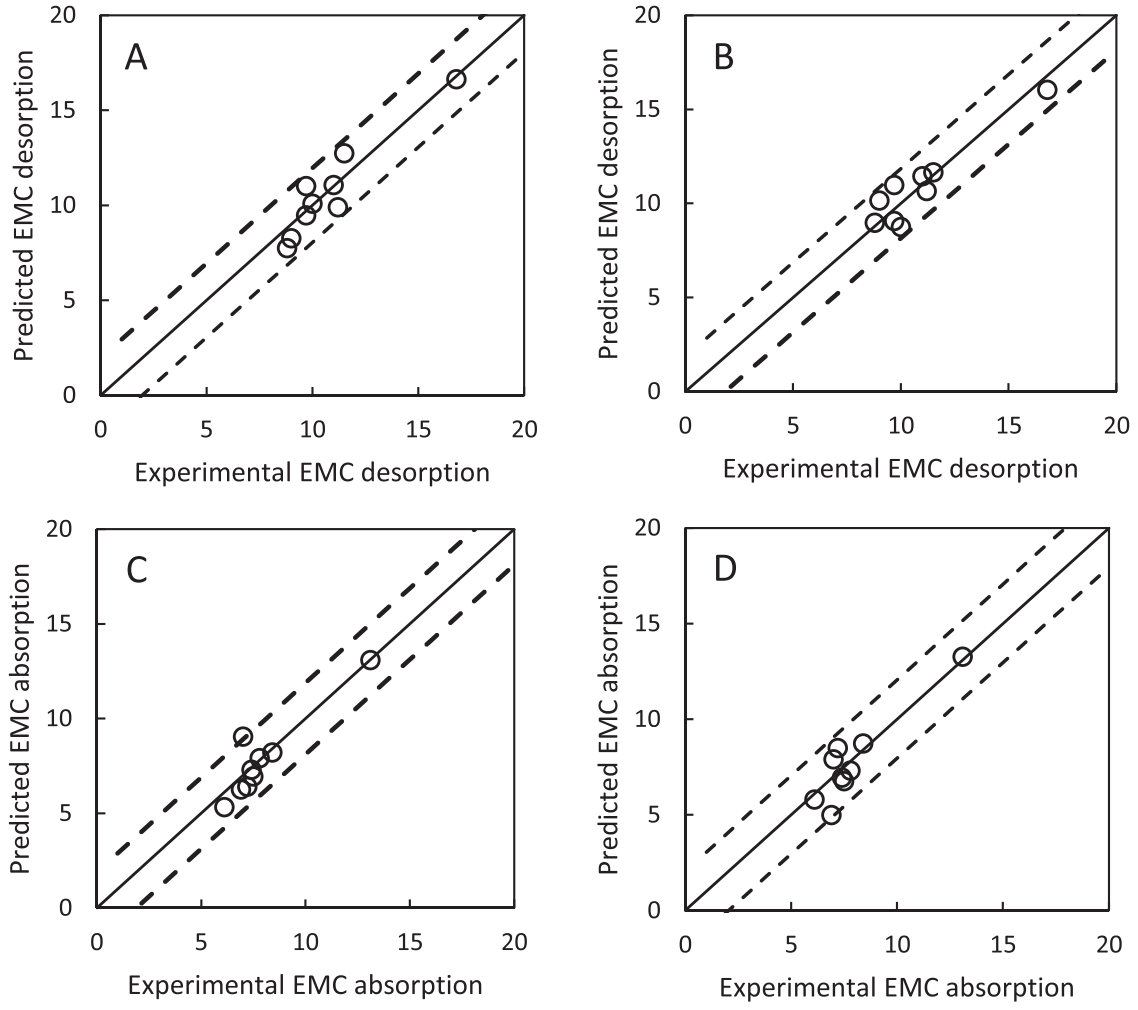

Fig. 3. Predicted versus actual EMC desorption and absorption (RH50). Dashed lines represent the RMSE (95%). A applied Eq. (3), C applied Eq. (4), B applied Eq. (5) and D applied Eq. (6).

$$EMC\ \ desorption\ \ = 0.0768\ \ \textbf{\textit{cellulose}}\ \ content + 0.3151\ \ hemicellulose\ \ content + 0.1106\ \ lignin\ \ content \quad (4)$$

$$EMC\ \ absorption\ \ = 0.1033\ \ \textbf{\textit{amorphous}}\ \ \textbf{\textit{cellulose}}\ \ content + 0.3111\ \ hemicellulose\ \ content + 0.0834\ \ lignin\ \ content \quad (5)$$

$$EMC\ \ absorption\ \ = 0.05843\ \ \textbf{\textit{cellulose}}\ \ content + 0.3145\ \ hemicellulose\ \ content \quad (6)$$

The accuracy of the model was validated by (i) calculating the correlation coefficients of the developed models and (ii) plotting the model predicted values against the experimental values. Based on the correlation coefficients (Table 4), all proposed models (Eqs. 3–6) are significant. The coefficients of determination (adj R^2) are all $\geq$ 98% which means that $\geq$ 98% of the variability in the responses (absorption/desorption) is explained for the region studied. Although all fits show high R^2 and adjusted R^2 values, caution should be taken since less than 10 data points were used to fit the equations. The goodness of fit of the models is also graphically assessed in Fig. 3. By plotting predicted values against experimental values, data points should approach the diagonal of the graph for a good fit. The confidence interval (CI) is defined by Eq. (8) and 9. This statistical procedure was performed for all proposed models (Eqs. 3–6). Most of the values are within the 95% RMSE band, implying an overall good model prediction (Fig. 3).

$$RMSE = \sqrt{\frac{\sum_{j=i}^{n} \left(P_j - E_i\right)^2}{n}} \quad (7)$$

$$CI = \quad \overline{x} \pm t_{95} * RMSE \quad (8)$$

RMSE represents the Root Mean Square Error, P_j; the predicted value of an experiment, E_i; the experimental value of an experiment, n; number of experiments, ($\overline{x}$); the mean value of a unique experiment, t_{95}; the t value of the inverse two-sided Student-t distribution for a confidence level of 95%.

Because of the small dataset it is difficult to draw conclusions about the true predictability for the EMC. One could think of complementary experiments to verify the moisture uptake of each constituent, by first splitting the fibre into its cellulose, hemicellulose and lignin fraction. However, separation of these components may alter their chemical structure, thereby affecting their moisture sorption behaviour (Kelley et al., 1987).

Another remark should be made, that although the moisture sorption of the fibres seems largely determined by their chemical composition, their composite properties in moist environment are controlled by other phenomena. As pointed out in the introduction, bamboo fibres may have a higher EMC when conditioned at a certain RH, than for example flax fibres; however their mechanical properties will be higher in a moist environment. This is controlled by the difference in plasticisation of the different chemical constituents present in the fibre (Back and Salmen, 1982). For this particular example, it was demonstrated that the high lignin content, present in bamboo fibres, helps the fibre to retain its structural integrity in moist environment.

4. Conclusion

Nine materials (flax, hemp, jute, spruce, bamboo, corn stalks, palm leaves, rice husk and wheat straw were gathered, potentially usable as a natural fibre in material applications. The adapted van Soest method used for the chemical composition analysis of the fibres was proven to be accurate and the obtained crystallinity data was realistic in comparison with the cellulose content enabling the effective determination of the non-crystalline cellulose content and its subsequent incorporation in the model. The developed models show that hemicellulose is the main contributor for both the water absorption and desorption process. It is also proven that non-crystalline cellulose, with its nano-porous structure and exposed hydroxyl sites, affects the sorption process significantly more compared to the overall cellulose content, which seems to be logical given the level of hydrophilicity of cellulose and the moisture inertness of crystalline cellulose. The experimental results of both moisture desorption and absorption for both cellulose and amorphous cellulose are compared to the theoretical values predicted by the linear regression models. The goodness of the fit of the models was shown by the correlation coefficients of the models (R^2 and adj R^2) that were $\geq$ 98% and a narrow distribution around the diagonal (slope 1) of the predicted versus experimental data graph. Although this study gains useful insights in the relation between chemical composition, crystallinity and sorption properties, further investigation is recommended. A larger dataset with more varying chemical compositions would be beneficial and/or physical and chemical properties of the individual cell wall constituents should be investigated separately. The latter is considered to be extremely difficult because through the (chemical) extraction and separation of these components, their chemical structure would be altered, and the moisture sorption behaviour would change accordingly.

CRediT authorship contribution statement

Nick Sweygers: Writing, Editing, Data curation, Methodology, Conceptualization. **Delphine E.C. Depuydt:** Writing, Editing, Data curation, Methodology, Conceptualization. **Samuel Eyley:** Data curation, Writing, Methodology regarding crystallinity measurements. **Wim Thielemans:** Supervision crystallinity measurements, editing. **Yasmine Mosleh:** Data curation DVS measurements, Writing and editing. **Jan Ivens:** Supervision, Writing, editing. **Raf Dewil:** Supervision. **Lise Appels:** Supervision, Writing and editing **Aart Willem Van Vuure**: Supervision, Methodology, Writing, Editing, Conceptualization.

Declaration of Competing Interest

The authors declare that they have no known competing financial interests or personal relationships that could have appeared to influence the work reported in this paper.

Acknowledgements

The authors would like to acknowledge the support of the Impulse Fund KU Leuven (BOF/IMP14/034) (Belgium). SE and WT greatly acknowledge the financial support through the Accelerate^3 project from the Interreg Vlaanderen-Nederland program and Flanders Innovation & Entrepreneurship for SWAXS. WT also thanks the Provincie West-Vlaanderen (Belgium) for financial support through his Province Chair in Advanced Materials.

References

Adam, A.B.A., Basta, A.H., El-Saied, H., 2018. Evaluation of palm fiber components an alternative biomass wastes for medium density fiberboard manufacturing. Maderas Cienc. Y Tecnol. 20, 579–594.
Ahmad, T., Rafatullah, M., Ghazali, A., Sulaiman, O., Hashim, R., 2011. Oil palm biomass-based adsorbents for the removal of water pollutantsa review. J. Environ. Sci. Heal. - Part C. Environ. Carcinog. Ecotoxicol. Rev. 29, 177–222.
Ahvenainen, P., Kontro, I., Svedström, K., 2016. Comparison of sample crystallinity determination methods by X-ray diffraction for challenging cellulose I materials. Cellulose 23, 1073–1086.
Arnata, I.W., Suprihatin, S., Fahma, F., Richana, N., Candra, T., 2019. Sunarti, cellulose production from sago frond with alkaline delignification and bleaching on various types of bleach agents. Orient. J. Chem. 35, 08–19.
Azwa, Z.N., Yousif, B.F., Manalo, A.C., Karunasena, W., 2013. A review on the degradability of polymeric composites based on natural fibres. Mater. Des. 47, 424–442.
Back, E.L., Salmen, N.L., 1982. Glass transitions of wood components hold implications for molding and pulping processes. Tappi 65, 107–110.
Baillie, C., 2000. Green composites, polymer composites and the environment. Woodhead Publising Limited, Cambridge, England.
Bashar, M.M., Zhu, H., Yamamoto, S., Mitsuishi, M., 2019. Highly carboxylated and crystalline cellulose nanocrystals from jute fiber by facile ammonium persulfate oxidation. Cellulose 26, 3671–3684.
Biswal, P., Patel, N., Samal, A.K., Rao, M., 2019. Investigation on mechanical properties of pondash/natural fiber based geopolymeric products. Int. J. Res. Anal. Rev. 6, 324–332.
Blackwell, P., Walker, J.C.F., 2006. Primary Wood Processing: Principles and Practice. Springer, Dordrecht, Netherlands.
Bourmaud, A., Beaugrand, J., Shah, D.U., Placet, V., Baley, C., 2018. Towards the design of high-performance plant fibre composites. Prog. Mater. Sci. 97, 347–408.
Cermák, P., Baar, J., Dömény, J., Výbohová, E., Rousek, R., Paril, P., Oberle, A., Abalová, I.G., Hess, D., Vodák, M., Brabec, M., 2022. Wood-water interactions of thermally modified, acetylated and melamine formaldehyde resin impregnated beech wood. Holzforschung 76, 437–450.
Chand, N., Fahim, M., 2008. Tribology of natural fiber polymer composites, Tribol. Nat. Fiber Polym. Compos. 1–205.
Chen, D., Zhou, J., Zhang, Q., Zhu, X., Lu, Q., 2014. Upgrading of rice husk by torrefaction and its influence on the fuel properties. BioResources 9, 5893–5905.
Cheng, P., Wang, K., Chen, X., Wang, J., Peng, Y., Ahzi, S., Chen, C., 2021. Interfacial and mechanical properties of continuous ramie fiber reinforced biocomposites fabricated by in-situ impregnated 3D printing. Ind. Crops Prod. 170, 113760.
De Figueiredo, L.P., Ferreira, F.F., 2014. The Rietveld Method as a Tool to Quantify the Amorphous Amount of Microcrystalline Cellulose. J. Pharm. Sci. 103, 1394–1399.
Douglas, D.S., Qinglin, W., Guangping, H., Christian, V.S., 2013. Introduction to Wood and Natural Fiber Composites. John Wiley & Sons, Inc, West Sussex, United Kingdom.
Effendi, E.Z., Hariady, Y.C., Salaahuddin, M.D., Irawan, C., Nata, I.F., 2019. Utilization of rice husk cellulose as a magnetic nanoparticle biocomposite fiber source for the absorption of manganese (Mn2+) ions in peat water. J. Kim. Sains Dan. Apl. 22, 220–226.
Engelund, E.T., Thygesen, L.G., Svensson, S., Hill, C.A.S., 2013. A critical discussion of the physics of wood-water interactions. Wood Sci. Technol. 47, 141–161.
Faruk, O., Bledzki, A.K., Fink, H.P., Sain, M., 2014. Progress report on natural fiber reinforced composites. Macromol. Mater. Eng. 299, 9–26.
Giummarella, N., Lawoko, M., 2016. Structural basis for the formation and regulation of Lignin-Xylan Bonds in Birch. ACS Sustain. Chem. Eng. 4, 5319–5326.
Govil, T., Saxena, P., Samanta, D., Singh, S.S., Kumar, S., Salem, D.R., Sani, R.K., 2020. Adaptive enrichment of a thermophilic bacterial isolate for enhanced enzymatic activity. Microorganisms 8, 1–16.
Gullón, P., Salazar, N., Muñoz, M.J.G., Gueimonde, M., Ruas-Madiedo, P., de los Reyes-Gavilán, C.G., Parajó, J.C., 2011. Assessment on the fermentability of xylooligosaccharides from rice husks. BioResources 6, 3096–3114.
Guo, T., Li, X., Liu, X., Guo, Y., Wang, Y., 2018. Catalytic transformation of lignocellulosic biomass into arenes, 5-hydroxymethylfurfural, and furfural. ChemSusChem 11, 2758–2765.
Gupta, M.K., Srivastava, R.K., 2015. Effect of sisal fibre loading on dynamic mechanical analysis and water absorption behaviour of jute fibre epoxy composite. Mater. Today Proc. 2, 2909–2917.
Hamdan, N.T., 2020. Investigation of crystallinity characterization of bamboo fibers using xylanase from aspergillus nidulans. Syst. Rev. Pharm. 11, 6–9.
Hill, A.S.C., Norton, A., Newman, G., 2009. The Water Vapor Sorption behavior of Natural Fibers. J. Appl. Polym. Sci. 112, 1524–1537.
Horvath, B., Peralta, P., Frazier, C., Peszlen, I., 2011. Thermal softening of transgenic aspen. BioResources 6, 2125–2134.
J.G, CELC, Flax & Hemp Fiber Composites, a market reality - The biobased solutions for the industry, 2018.
João, J.J., Locks, L., Vieira, J.L., Lucia, E.A., 2020. Rice husks as a microbial source for wastewater treatment. Rev. Bras. Eng. Agric. E Ambient. 24, 343–347.
John, M., Sabu, T., 2012. Natural Polymers. In: Composites, Volume 1. The Royal Society of Chemistry, Cambridge England.
Kabir, M.M., Wang, H., Lau, K.T., Cardona, F., 2012. Chemical treatments on plant-based natural fibre reinforced polymer composites: An overview. Compos. Part B Eng. 43, 2883–2892.
Kelley, S.S., Rials, T.G., Glasser, W.G., 1987. Relaxation behaviour of the amorphous components of wood. J. Mater. Sci. 22, 617–624.
Khattab, M.S.A., El, A.M.A., 2018. Tawab, In vitro evaluation of palm fronds as feedstuff on ruminal digestibility and gas production. Acta Sci. - Anim. Sci. 40.
Ku, C.S., Jang, J.P., Mun, S.P., 2007. Exploitation of polyphenol-rich pine barks for potent antioxidant activity. J. Wood Sci. 53, 524–528.
Kumar, S., 2018. Fabrication and analysis of thermocol sandwiched between bamboo fiber-reinforced phenol formaldehyde composite laminates. Int. J. Res. Adv. Dev. © Ijrad. 1, 130–134.
Lawoko, M., Henriksson, G., Gellerstedt, G., 2005. Structural differences between the lignin-carbohydrate complexes present in wood and in chemical pulps. Biomacromolecules 6, 3467–3473.
Le Normand, M., Moriana, R., Ek, M., 2014. Isolation and characterization of cellulose nanocrystals from spruce bark in a biorefinery perspective. Carbohydr. Polym. 111, 979–987.
Leenakul, W., Tippayawong, N., 2010. Dilute acid pretreatment of bamboo for fermentable sugar production. J. Sustain. Energy Environ. 1, 117–120.
Lindner, M., 2018. Factors affecting the hygroexpansion of paper. J. Mater. Sci. 53, 1–26.
Liu, Y., Xie, J., Wu, N., Ma, Y., Menon, C., Tong, J., 2019. Characterization of natural cellulose fiber from corn stalk waste subjected to different surface treatments. Cellulose 26, 4707–4719.
Liu, Z., Tisserat, B.H., 2018. Coating applications to natural fiber composites to improve their physical, surface and water absorption characters. Ind. Crops Prod. 112, 196–199.
Liuzzi, S., Rubino, C., Martellotta, F., Stefanizzi, P., Casavola, C., Pappalettera, G., 2020. Characterization of biomass-based materials for building applications: the case of straw and olive tree waste. Ind. Crops Prod. 147, 112229.
Lu, D., Xiao, K., Chen, Y., Soh, Y.N.A., Zhou, Y., 2018. Transformation of dissolved organic matters produced from alkaline-ultrasonic sludge pretreatment in anaerobic digestion: From macro to micro. Water Res 142, 138–146.
Manian, A.P., Cordin, M., Pham, T., 2021. Extraction of cellulose fibers from flax and hemp: a review. Cellulose 28, 8275–8294.
Monavari, S., Galbe, M., Zacchi, G., 2009. The influence of solid/liquid separation techniques on the sugar yield in two-step dilute acid hydrolysis of softwood followed by enzymatic hydrolysis. Biotechnol. Biofuels. 2, 1–9.
S. Morin, S. Prof, A. Richel, Study of chemical and enzymatic functionalization of lignocellulosic natural fibers Designing natural fibers for biocomposites. PhD (2021) 1–305.
Moryganov, A.P., Zavadskii, A.E., Stokozenko, V.G., 2018. Special Features of X-ray Analysis of Cellulose Crystallinity and Content in Flax Fibres. Fibre Chem. 49, 382–387.
Müssig, J., 2010. Industrial Applications of Natural Fibres. John Wiley & Sons, Inc, West Sussex, United Kingdom.
Mwaikambo, L.Y., Ansell, M.P., 2002. Chemical modification of hemp, sisal, jute, and kapok fibers by alkalization. J. Appl. Polym. Sci. 84, 2222–2234.
Nasser, R.A., Salem, M.Z.M., Hiziroglu, S., Al-Mefarrej, H.A., Mohareb, A.S., Alam, M., Aref, I.M., 2016. Chemical analysis of different parts of date palm (Phoenix dactylifera L.) using ultimate, proximate and thermo-gravimetric techniques for energy production. Energies 9.
Nishiyama, Y., Sugiyama, J., Chanzy, H., Langan, P., 2003. Crystal structure and hydrogen bonding system in cellulose iα from synchrotron X-ray and neutron fiber diffraction. J. Am. Chem. Soc. 125, 14300–14306.
Owolabi, A.F., Ghazali, A., Khalil, H.P.S.A., Hassan, A., Arjmandi, R., Fazita, M.R.N., Haafiz, M.K.M., 2016. Isolation and characterization of microcrystalline cellulose from oil palm fronds using chemomechanical process. Wood Fiber Sci. 48, 260–270.
Özyürek, Ö., van Heiningen, A., 2018. Formic acid reinforced autohydrolysis of wheat straw for high yield production of monosugars and minimal lignin precipitation. Ind. Crops Prod. 112, 320–326.
Park, S., Baker, O.J., Himmel, E.M., Parilla, A.P., Johnson, K.D., 2010. Research Cellulose crystallinity index: measurement techniques and their impact on interpreting cellulase. Biotechnol. Biofuels. 3, 1–10.
Rautkari, L., Hill, C.A.S., Curling, S., Jalaludin, Z., Ormondroyd, G., 2013. What is the role of the accessibility of wood hydroxyl groups in controlling moisture content? J. Mater. Sci. 48.

Rowell, R.R., 2005. Handbook of Wood Chemistry and Wood Composites. Taylor & Francis Group, Boca Raton, USA.
Salmén, L., 2015. Wood morphology and properties from molecular perspectives. Ann. . Sci. 72, 679–684.
Salmén, L., Bergström, E., 2009. Cellulose structural arrangement in relation to spectral changes in tensile loading FTIR. Cellulose 16, 975–982.
Savic, A., Antonijevic, D., Jelic, I., Zakic, D., 2020. Thermomechanical behavior of bio-fiber composite thermal insulation panels. Energy Build. 229, 110511.
Shahinur, S., Sayeed, M.M.A., Hasan, M., Sadat, A., Sayem, M., Haider, J., Ura, S., 2022. Current Development and Future Perspective on Natural Jute Fibers and Their Biocomposites. Polymers 14, 1445.
Shmulsky, R., Jones, P.D., 2011. Forest Products and Wood Science An Introduction, Sixth edition.,. John Wiley & Sons, Inc, West Sussex United Kingdom.
Skulcova, A., Haščičova, Z., Hrdlička, L., Sima, J., Jablonsky, M., 2018. Green solvents based on choline chloride for the extraction of spruce bark (Picea abies). Cellul. Chem. Technol. 52, 171–179.
Stevulova, N., Cigasova, J., Estokova, A., Terpakova, E., Geffert, A., Kacik, F., Singovszka, E., Holub, M., 2014. Properties characterization of chemically modified hemp hurds. Mater. (Basel) 7, 8131–8150.
N. Sweygers, R. Dewil, L. Appels, The generalized analysis of lignocellulosic fraction in biomass (article in prepartion for submission).
Sweygers, N., Somers, M.H., Appels, L., 2018. Optimization of hydrothermal conversion of bamboo (Phyllostachys aureosulcata) to levulinic acid via response surface methodology. J. Environ. Manag. 219, 95–102.
T. A, Abdul, F., 2013. Cellulose microfibril angle in wood and its dynamic mechanical significance. Cellul. - Fundam. Asp.
Terinte, N., Ibbett, R., Schuster, K.C., 2017. Overview on native cellulose and microcrystalline cellulose I structure studied by X-ray diffraction (WAXD): comparison between measurement techniques. Lenzing. Ber. 89, 118–131.
Thygesen, A., Oddershede, J., Lilholt, H., Thomsen, A.B., Ståhl, K., 2005. On the determination of crystallinity and cellulose content in plant fibres. Cellulose 12, 563–576.
Time, B., 1998. Hygroscopic moisture transport in wood. Dep. Build. Constr. Eng. PhD 1–232.
Tozluoğlu, A., Özyürek, Ö., Çöpür, Y., Özdemir, H., 2015. Papermak. Pulp Wheat Straw 10, 7834–7853.
Vahtikari, K., Rautkari, L., Noponen, T., Lillqvist, K., 2017. (née Laine), M. Hughes, The influence of extractives on the sorption characteristics of Scots pine (Pinus sylvestris L.). J. Mater. Sci. 52, 10840–10852.
Wang, X., Cheng, D., Huang, X., Song, L., Gu, W., Liang, X., Li, Y., Xu, B., 2020. Effect of high-temperature saturated steam treatment on the physical, chemical, and mechanical properties of moso bamboo. J. Wood Sci. 66.
Wei, X., Yuan, J., Wang, G., Chen, F., Chen, X., Jiang, H., Smith, L.M., Deng, J., 2022. Effect of chemical composition and cell structure on water vapor sorption behavior of parenchyma cells and fiber cells in moso bamboo (Phyllostachys edulis). Ind. Crops Prod. 178, 114652.
Yang, T., Zhou, H., Ma, E., Wang, J., 2018. Effects of removal of different chemical components on moisture sorption property of Populus euramericana Cv. under dynamic hygrothermal conditions. Results Phys. 10, 61–68.
Yao, C., Tian, X., Sheng, C., 2019. Moisture sorption isotherm of herbaceous an agricultural biomass. Energy Fuels 33, 12480–12491.
Yelle, D.J., Kaparaju, P., Hunt, C.G., Hirth, K., Kim, H., Ralph, J., Felby, C., 2013. Two-dimensional NMR evidence for cleavage of lignin and xylan substituents in wheat straw through hydrothermal pretreatment and enzymatic hydrolysis. Bioenergy Res. 6, 211–221.
Young, R.A., 1985. The chemistry of solid wood. Wood Sci. Technol. 19, 17–18.
Zevin, L.S., Kimmel, G., 1995. Quantitative X-Ray Diffractometry, Quant. X-Ray Diffractometry. Springer,, Dordrecht, Netherlands.
Zhou, H., Xu, R., Ma, E., 2016. Effects of removal of chemical components on moisture adsorption by wood. BioResources 11, 3110–3122.